

Electron Injection/Transport Mechanism in OLEDs Unraveled by Producing Ultralow-Work-Function Electrodes

Hirohiko Fukagawa

fukagawa.h-fe@nhk.or.jp

NHK, 1-10-11 Kinuta, Setagaya-ku, Tokyo 157-8510, Japan

Keywords: Electron injection, Hydrogen bond, Coordination reaction, Work function

ABSTRACT

It was found that the work function of aluminum can be reduced to about 2.0 eV by utilizing a superbases. This extremely low work function enabled us to gain a complete understanding of the electron injection/transport mechanism in organic light-emitting diodes.

1. Introduction

Understanding the carrier injection and transport mechanisms in organic optoelectronic devices is of pivotal importance in their future development. However, much of the conventional wisdom about materials and device structures has been gained by evaluating the device characteristics through the development of numerous devices rather than the clarification of working mechanisms of devices [1–4]. Since the electron affinity (EA) of the materials used in organic light-emitting diodes (OLEDs) is smaller than that of the materials used in other organic devices, chemically reactive alkali elements such as Li and Cs have been essential for the electron injection layer (EIL) near the cathode [2,5]. In addition, compounds with nitrogen-containing heterocycles, such as pyridine, imidazole, and phenanthroline, have been typically defined as electron transport materials (ETMs) and used as the electron transport layer (ETL) [3,4]. The use of both alkali elements and these typical ETMs is now almost seen as conventional wisdom that has been gained through the development of numerous OLEDs; however, the detailed mechanisms involved in electron injection/transport from the cathode to the emitting layer (EML) have remained unclear for more than 30 years. The effect of the electron injection property on the operating voltage has rarely been discussed since little has been known about the actual EA of organic compounds with a small EA until recently [5].

Here, we have unraveled the electron injection/transport mechanism in OLEDs and redefined the materials/structures of OLEDs. The method of fabricating a low-work-function (WF) electrode without reactive alkali elements, which are widely used for electron injection, from organic devices has been the subject of intensive studies in recent years, as illustrated in Fig. 1 [6–11]. A research group from Georgia Institute of Technology developed electrodes with a WF of about 3 eV by utilizing polyethyleneimine (PEI) [6]. Very recently, a research group from National University of Singapore developed an electrode with a WF of 2.4 eV by using multivalent anions [7]. A research group from Tsinghua University and our group reported some phenanthroline derivatives that can reduce the WF of electrodes to below 3 eV by utilizing the coordination reaction from phenanthroline derivatives with metals [8,9]. We also demonstrated that the formation of hydrogen bonds (H-bonds) between nitrogen in bases and other organic semiconductors reduces the WF to about 3 eV [10,11]. The novel EIL found in this study is the superbases 2,6-bis(1,3,4,6,7,8-tetrahydro-2H-pyrimido[1,2-a]pyrimidin-1-yl)pyridine (Py-hpp₂) [12], which can reduce the WF near an Al cathode to about 2.0 eV through both the coordination reaction and the formation of H-bonds [13]. This extremely low WF allows direct electron injection even into materials used for a blue-emitting layer, and it was found that organic materials can transport electrons independently of their molecular structure. On the basis of these findings, a simply structured blue OLED with an operational lifetime of more than 1,000,000 hours is realized.

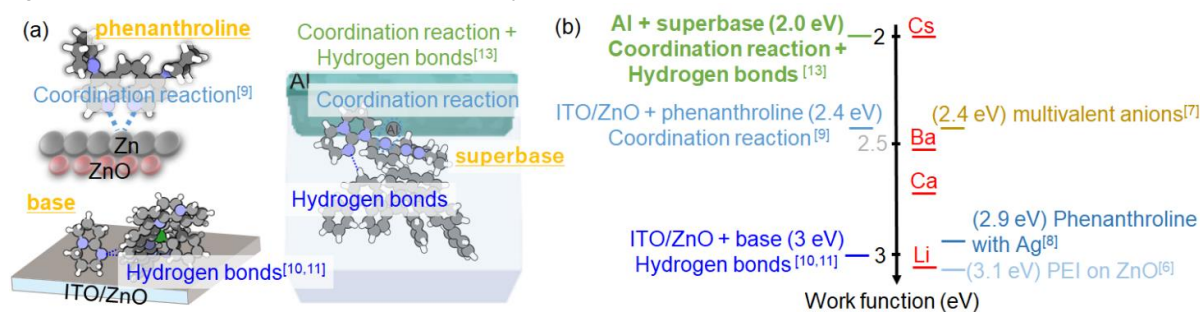


Figure 1: (a) Schematic illustration of chemical interactions related to WF tuning. (b) Summary of WFs tuned by chemical reactions.

2. Effect of electron injection barrier on operating voltage of OLEDs

The electron injection/transport mechanism was clarified by investigating the EIL- and ETL-dependent characteristics of green OLEDs, as shown in Fig. 2(a). Two similar materials were used for the ETL, as shown in Figs. 2(b) and 2(c): one was 7,10-bis(biphenyl-3-yl)-8,9-diphenylfluoranthene (F-Ph), which is an aromatic hydrocarbon, and the other was 7,10-bis(3-(pyridin-3-yl)phenyl)-8,9-diphenylfluoranthene (F-Py), which is considered to be a typical ETM owing to the existence of the pyridine substituent. There are no significant differences in EA measured by low-energy inverse photoemission spectroscopy (LEIPS). However, the operating voltage was found to be highly dependent on the material used in the ETL for the OLEDs without EIL and for the OLEDs with (8-quinolinolato)lithium (Liq), which is a typical EIL, as shown in Figs. 2(b) and 2(c). According to conventional wisdom, these results can be attributed to the electron transportability of F-Py being higher than that of F-Ph. Note the operating voltage is almost independent of the material used in the ETL when Py-hpp₂, which is the superbase, was used for the EIL. Thus, it may be presumed that F-Ph can transport electrons to the EML if electrons can be injected from the cathode to F-Ph.

To verify this hypothesis, the electron injection barriers (EIBs) at the Al/ETL interfaces of each OLED were investigated using a combination of LEIPS and ultraviolet photoelectron spectroscopy (UPS), as summarized from Figs. 2(d) to 2(h). It was found that the operating voltage strongly depends on the EIB, which is defined as the energy difference between WF around the cathode and the EA of the ETL. In the OLED with F-Ph/no EIL [Fig. 1(f)], the high EIB of about 1.56 eV is observed at the Al/F-Ph interface, which is consistent with the high operating

voltage of the OLED [Fig. 1(b), no EIL]. Since Li compounds such as Liq reduce the WF around the cathode simply because of their low charge neutrality level, the EIB at the Al/Liq/F-Ph interface is reduced to 1.05 eV [Fig. 1(e)] [14]. In the case of the Al/F-Py interface, it was clarified that the EIB is reduced significantly owing to the coordination reaction between pyridine in F-Py and Al atoms that diffuse into F-Py [5,8,9]. The change in WF originates from the coordination reaction (Δ_{co}), and the direct measurement of EA by LEIPS clarified that the coordination reaction also causes the change in the EA of F-Py from 2.16 eV to 2.80 eV (δ_{EA}) [Fig. 1(h)] [5,15]. Thus, it was found that the EIB can significantly be reduced by utilizing the coordination reaction. The EIB was found to be almost zero when Liq was inserted between Al and F-Py, resulting in the lowest operating voltage [Fig. 1(g)]. Note the EIB in OLED with Py-hpp₂ and F-Ph [Fig. 1(d)], the turn-on voltage of which is similar to that of OLED with Liq/F-Py. The insertion of Py-hpp₂ between Al and F-Ph reduces the WF to about 2.0 eV, resulting in an almost zero EIB. It was found that both the coordination reaction and the formation of H-bonds contribute to the decrease in WF. The deposition of 1-nm-thick Py-hpp₂ on F-Ph decreases the surface WF to about 2.5 eV owing to the formation of H-bonds [10]. The WF was further reduced to about 2.0 eV by utilizing the coordination reaction when Al was deposited on this film [8,9]. It was found that reducing the EIB to near zero seems to be essential for delivering electrons from the cathode to the EML at a low operating voltage. In addition, the results of our experiment suggest that nitrogen-containing heterocyclic compounds perform electron injection through the coordination reaction rather than electron transport.

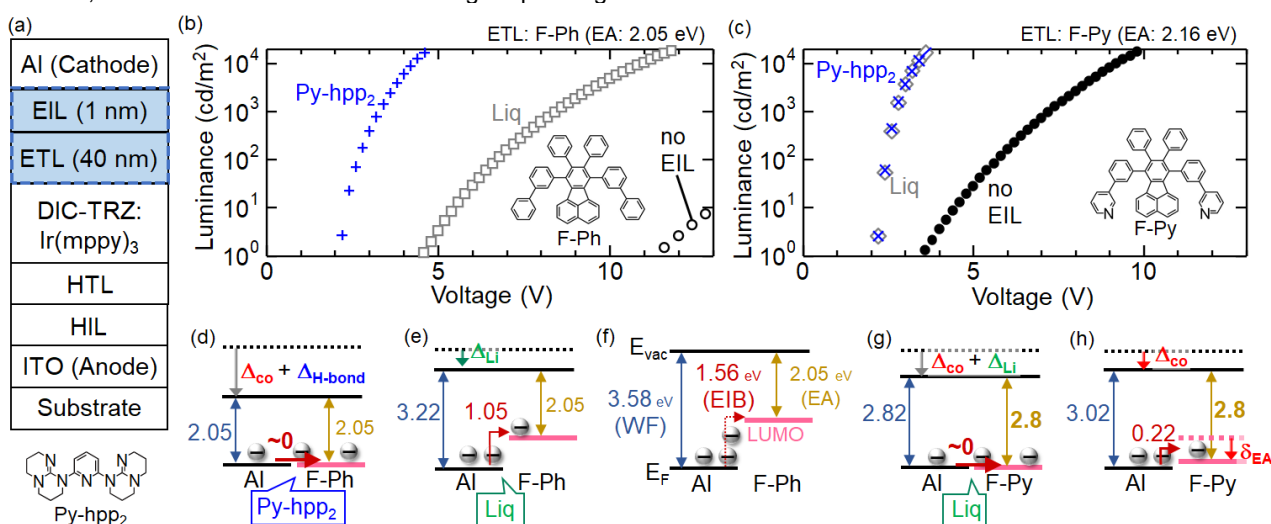


Figure 2: (a) Multilayer structure of an OLED, chemical structure of Py-hpp₂. (b,c) Luminance–voltage characteristics of green OLEDs prepared using various EIL/ETL combinations. Inset: chemical structure of the material used as ETL. (d)–(h) Summary of the energy diagrams around each cathode estimated from results of UPS and LEIPS, where E_F and E_{vac} are the Fermi and vacuum levels, respectively.

3. Simply structured green/blue OLEDs with high performances

It was found that the range of choices of materials used between the cathode and the EML is expected to be increased greatly by using Py-hpp₂. Based on our findings, we have succeeded in developing innovative green and blue OLEDs with low operating voltage, high efficiency, and high operational stability despite the simple device structure, as summarized from Figs. 3(a) to 3(i). The realization of an ultralow WF of about 2 eV enables direct electron injection into hosts of green phosphorescent OLEDs (PHOLEDs) and blue fluorescent OLEDs.

Figure 3(d) shows the luminance (*L*)–voltage (*V*) characteristics of green PHOLEDs prepared using three EIL/ETL combinations. An EIL-dependent operating voltage was clearly observed in green PHOLEDs, as shown in Figs. 3(a) and 3(d): the luminance of the green PHOLED with DIC-TRZ as the ETL was significantly increased by changing the EIL from LiF to Py-hpp₂. The *L*–*V* characteristics of the PHOLED with the Py-hpp₂/DIC-TRZ combination are comparable to those of the PHOLED with a typical EIL/ETL combination (LiF/B4PyMPM) [Fig. 3(b)]. The PHOLED with Py-hpp₂/DIC-TRZ exhibits an external quantum efficiency (EQE) of over 20% (not shown). In addition, the operational stability of the PHOLED with Py-hpp₂/DIC-TRZ is almost the same as that of the PHOLED with LiF/B4PyMPM, as shown in Fig.

3(e). Thus, long-lived PHOLEDs with low operating voltage and high efficiency could be realized without using typical ETMs.

An EIL-dependent operating voltage was clearly observed even in the simply structured blue fluorescent OLED, as shown in Figs. 3(f) and 3(h): the luminance of the blue OLED was increased by about 200,000 times at an applied voltage of 6 V by changing the EIL from Liq to Py-hpp₂. The blue OLED with Py-hpp₂ exhibits a high EQE of more than 9% (not shown). In addition, the blue OLED with Py-hpp₂ shows both good color purity and an extremely long operational lifetime, as shown in Figs. 3(h) and 3(i). Since the time required for the luminance to decay to 50% of the initial luminance of 100 cd/m², which is discussed as the lifetime for many blue OLEDs (LT50), is too long to be measured, we estimated the lifetime from the data shown in Fig. 3(i) [16–18]. The lifetime was estimated to be more than 1,000,000 h, which is almost the same as that of OLEDs used in commercial products [16]. The fact that a long-lived blue OLED could be realized without using typical ETMs is of great significance for the realization of highly efficient and long-lived blue OLEDs, which is at the frontier of OLED research. Py-hpp₂ will eliminate the need for a typical ETM with high triplet energy and stability, which is a bottleneck in realizing long-lived blue OLEDs fabricated using phosphorescent and TADF emitters [19].

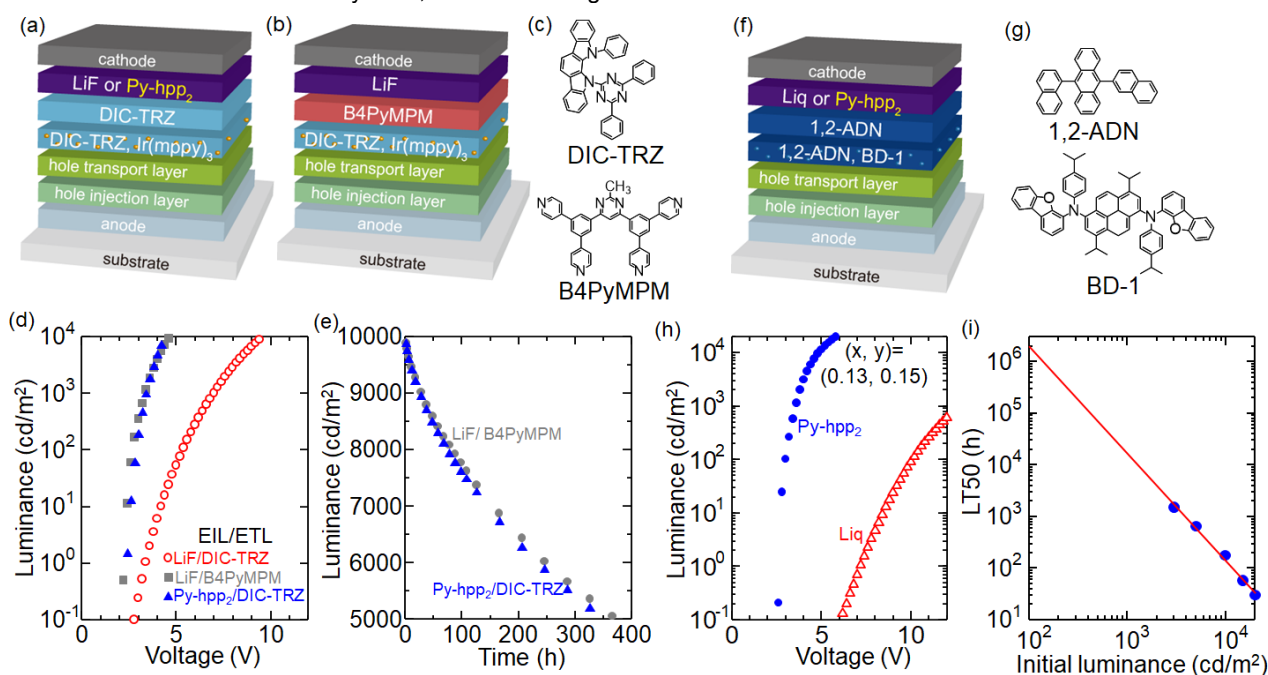


Figure 3. Schematic illustrations of (a) a simply structured green PHOLED and (b) a conventional PHOLED. (c) Chemical structure of the material used in PHOLEDs. (d) Luminance–voltage characteristics of green PHOLEDs prepared using various EIL/ETL combinations. (e) Luminance–time characteristics of PHOLEDs under a constant dc with an initial luminance of 10,000 cd/m². (f) Schematic illustration of a simply structured blue fluorescent OLED. (g) Chemical structure of the material used in fluorescent OLEDs. (h) Luminance–voltage characteristics of blue fluorescent OLEDs with different EILs. (i) Lifetime extrapolation for the blue OLED with Py-hpp₂. Data points are obtained at different initial luminance values.

4. Conclusion

We have unraveled the electron injection/transport mechanism in OLEDs by fabricating an ultralow-WF cathode. The reactive alkali elements and typical ETMs, such as compounds with nitrogen-containing heterocycles, are not essential for delivering electrons from the cathode to the EML in OLEDs if electrons can be injected effectively. Simply structured OLEDs with low operating voltage, high efficiency, and high operational stability were realized. The electron injection/transport mechanism unraveled in this study is expected to contribute to significant progress in the development of OLEDs.

Acknowledgement

Novel materials for EIL were co-developed with NIPPON SHOKUBAI CO., LTD.

REFERENCES

- [1] L. S. Hung, *et al.*, Appl. Phys. Lett. Vol. 70, p. 152 (1997).
- [2] X. Lin *et al.*, Nat. Mater. Vol. 16, p. 1209 (2017).
- [3] K. Walzer *et al.*, Chem. Rev. Vol. 107, p. 1233 (2007).
- [4] L. Xiao *et al.*, Adv. Mater. Vol. 23, p. 926 (2011).
- [5] H. Yoshida *et al.*, Org. Electron. Vol. 20, p. 24 (2015).
- [6] Y. Zhou *et al.*, Science Vol. 336, p. 327 (2012).
- [7] C. G. Tang *et al.*, Nature Vol. 573, p. 519 (2019).
- [8] Z. Bin *et al.*, Nat. Commun. Vol. 10, p. 866 (2019).
- [9] H. Fukagawa *et al.*, Nat. Commun. Vol. 11, p. 3700 (2020).
- [10] H. Fukagawa *et al.*, Adv. Mater. Vol. 31, p. e1904201 (2019).
- [11] H. Fukagawa *et al.*, Proc. IDW '19, p. 840 (2019).
- [12] R. J. Schwamm *et al.*, J. Org. Chem. Vol. 81, p. 7612 (2016).
- [13] T. Sasaki and H. Fukagawa *et al.*, Nat. Commun. Vol. 12, p. 2706 (2021).
- [14] S. Park, *et al.*, Chem. Phys. Lett. Vol. 652, p. 102 (2016).
- [15] Y. Isshiki *et al.*, J. Am. Chem. Soc. Vol. 140, p.3760 (2018).
- [16] Y. Zhang *et al.*, Nat. Commun. Vol. 5, p. 5008 (2014).
- [17] C. Féry *et al.*, Appl. Phys. Lett. Vol. 87, p. 213502 (2005).
- [18] E. Orselli *et al.*, Org. Electron. Vol. 13, p. 1506 (2012).
- [19] Y. Kondo *et al.*, Nat. Photon. Vol. 13, p. 678 (2019).